Electronic Supplementary Material (ESI) for Journal of Materials Chemistry A.

Supporting Information for

Solving the puzzle of $Li_4Ti_5O_{12}$ surface reactivity in aprotic electrolytes in Li-ion batteries by nanoscale XPEEM spectromicroscopy

Daniela Leanza [a], Carlos A. F. Vaz[b], Izabela Czekaj[c], Petr Novák [a], Mario El Kazzi*, [a]

[a] Paul Scherrer Institut, Electrochemistry Laboratory, 5232 Villigen PSI, Switzerland

[b] Paul Scherrer Institut, Swiss Light Source, 5232 Villigen PSI, Switzerland.

[c] Faculty of Chemical Engineering and Technology, Cracow University of Technology, Cracow, Poland

*Correspondence to: mario.el-kazzi@psi.ch

This PDF file includes:

Supplementary Text
Figures S1 to S11
Tables S1 to S2

Supplementary Text

The respective reversible lithiation/delithiation reactions during charge and discharge of $LiFePO_4$ and $Li_4Ti_5O_{12}$ are described by the equation S1 and S2, respectively:

$LiFe^{2+}PO_4 - Li^+ - e^- \rightarrow Fe^{3+}PO_4$ (equation S1)

$Li_4Ti_5^{4+}O_{12} + 3\ Li^+ + 3e- \rightarrow Li_7\ [Ti_2^{4+}Ti_3^{3+}]O_{12}$ (equation S2)

Those reactions show that during LFPO delithiation Fe^{2+} is oxidized to Fe^{3+} and during L4TO lithiation $3Ti^{4+}$ per unit formula are normally reduced to Ti^{3+}.

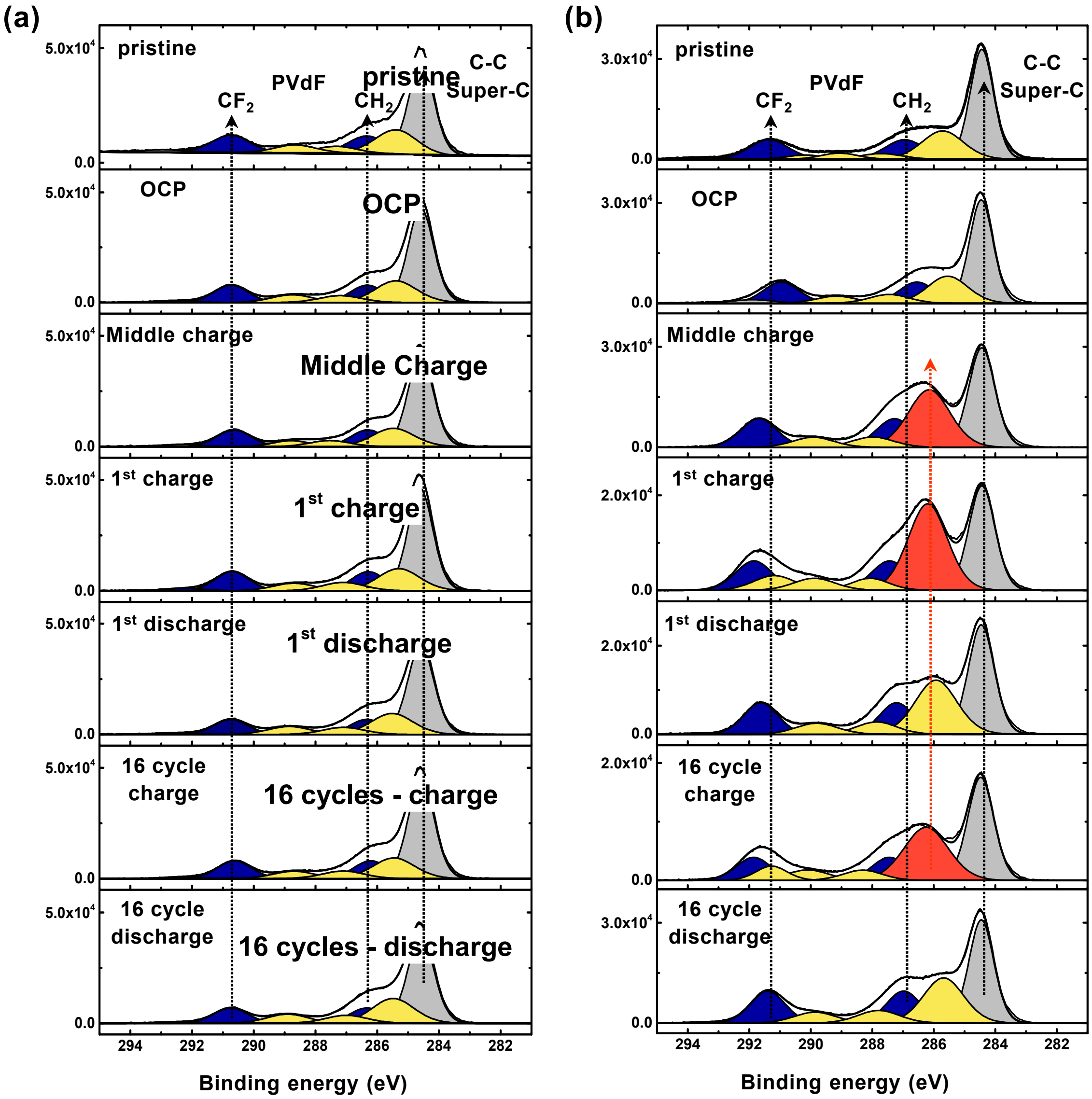

Fig. S1. XPS C1s core levels acquired on LFPO (a) and L4TO (b) for the pristine electrodes and electrodes at open circuit potential (OCP) and at different potentials after being cycled at C/5 in LC30 electrolyte. The electrodes formulation is 80% active materials, 10% conductive carbon and 10% PVdF binder.

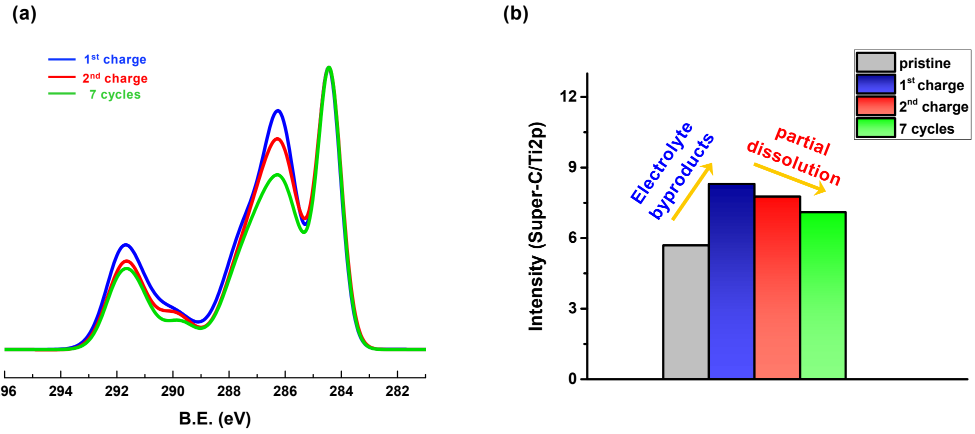

Fig. S2. (a) XPS C1s core levels acquired on lithiated L7TO electrodes after the 1st charge (blue); 2nd charge (red); 7 cycles (green). (b) Intensity ratio between the signals of Super-C (C-C) and Ti2p to follow the evolution of surface layer on top of the active material and conductive carbon in the lithiated L7TO samples. The electrodes formulation is 80% active materials, 10% conductive carbon and 10% PVdF binder.

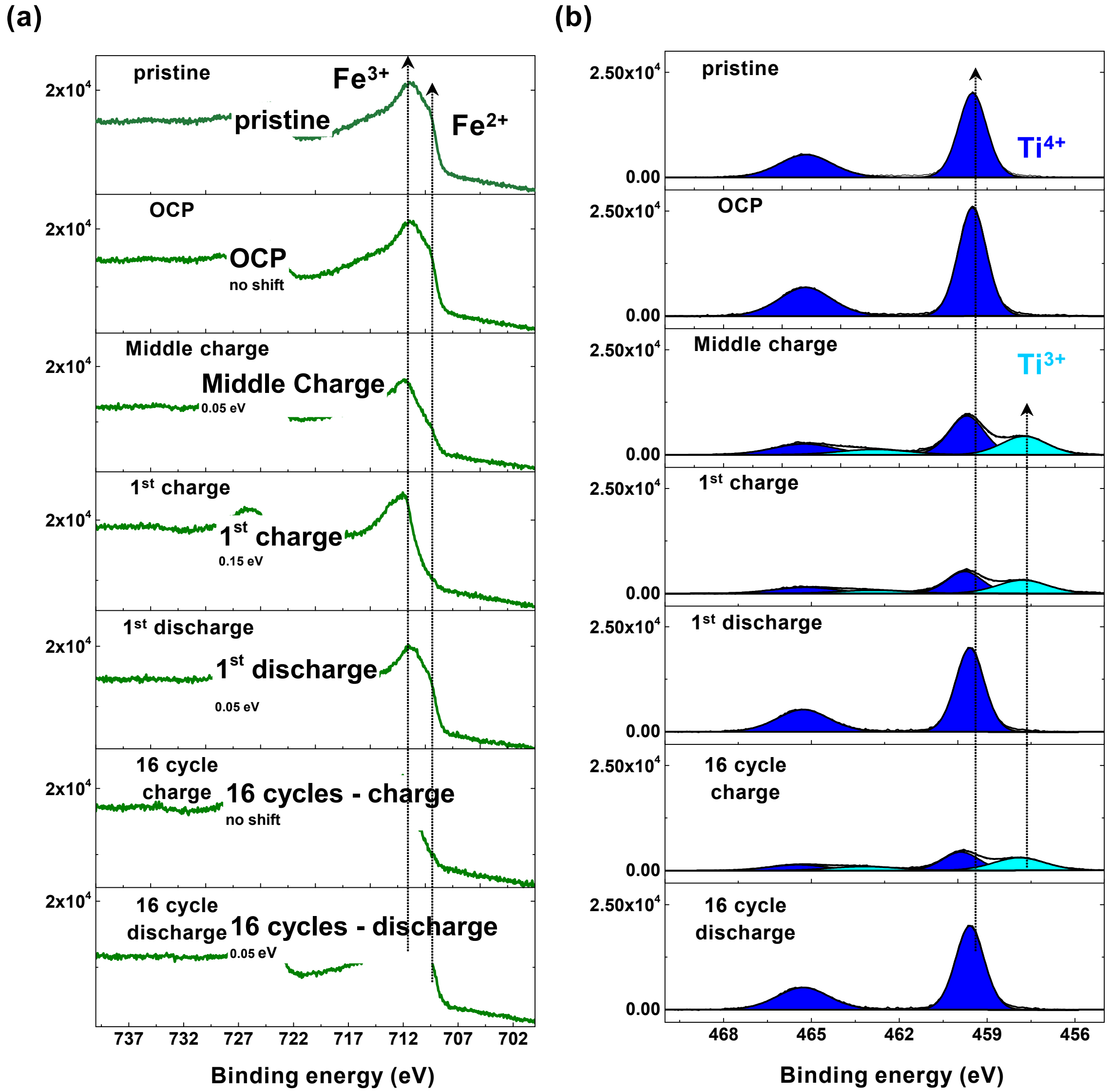

Fig. S3. XPS core levels of Fe2p (a) and Ti2p (b) acquired respectively on LFPO and L4TO electrodes in pristine state, at OCP and after different stages of cycling, to probe their electrochemical behavior after charge/discharge. The electrodes formulation is 80% active materials, 10% conductive carbon and 10% PVdF binder.

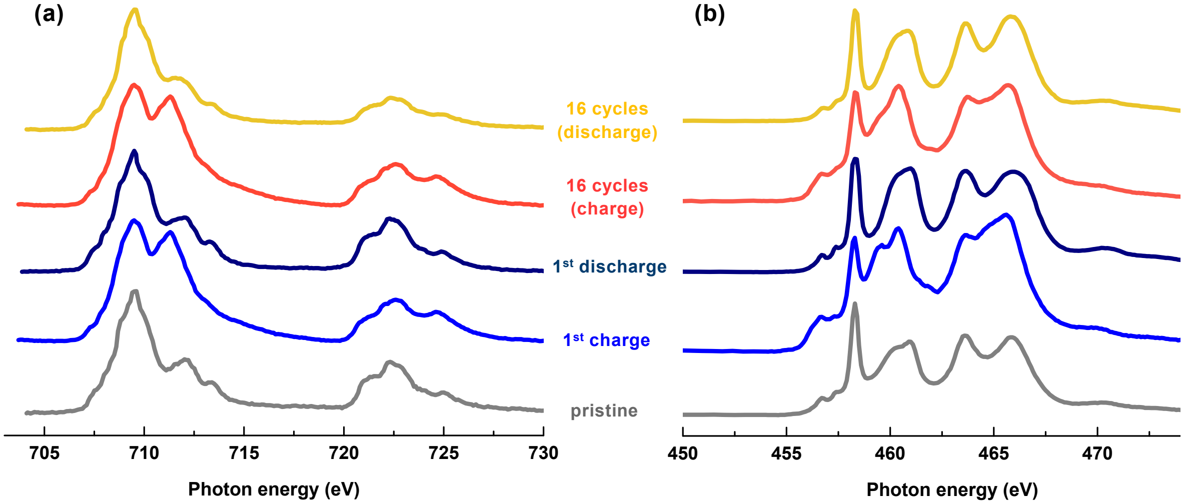

Fig. S4. Local XAS measurements performed at the Fe (a) and Ti (b) L-edges on LFPO and L4TO electrodes in pristine state and cycled electrodes after different stage of charge/discharge. The electrodes formulation is 80% active materials, 10% conductive carbon and 10% PVdF binder.

Figure S5 shows optimized structures of the investigated solvents DMC and EC and figures S6 and S7 display clusters representing the structure of the delithiated $FePO_4$ (referred to FPO) and lithiated $LiFePO_4$ (referred to LFPO), non-lithiated $Li_4Ti_5O_{12}$ (referred to L4TO) and lithiated $Li_7Ti_5O_{12}$ (referred to L7TO), respectively. In DMC and EC adsorption studies we take advantage of the localized interactions in cluster models. Despite some limitations (e.g. the parameters can depend on size and geometry of clusters), the problem of strong interactions between artificial surface layers, high artificial coverage of adsorbates or the influence of surface termination on the interaction between artificial surface layers is avoided, in contrast to periodic calculations. One fundamental challenge of clusters model calculation is the embedding problem (coming from artificial OH groups at the periphery of clusters), which has been avoided here by considering several clusters with different size (only the largest clusters are shown in the paper). In cluster model the adsorption process is defined locally, therefore less surface centres should be considered as responsible for adsorption process. The clusters of LFPO and L4TO have been cut from crystals with the following crystallographic parameters. The FPO is described by the space group Pnma (No. 62) with lattice constants a = 9.8142 Å, b = 5.7893 Å, c = 4.7820 Å. The crystal unit cell contains Fe at positions 4c, P at positions 4c, and O at positions 4c and 8d. The LFPO is described by the space group Pnma (No. 62) with lattice constants a = 10.3290 Å, b = 6.0065 Å, c = 4.6908 Å. The crystal unit cell contains Fe at positions 4c, P at positions 4c, and O at positions 4c and 8d as well as Li at positions 4a. The L4TO is described by the space group F d -3 m Z (No. 227) with lattice constant a = b = c = 8.35876 Å. The crystal unit cell contains Li at positions 8a, Ti at positions 16d and O at positions 32e. The partially lithiated L7TO is described by the space group F d -3 m Z (No. 227) with lattice constant a = b = c = 8.346 Å. The crystal unit cell contains two types of Li at the positions 8a and 16c, Ti at positions 16d and O at positions 32e. The LTO (100) surface is constructed by the lateral Ti-O layer (lateral distance between O and Ti is equal 0.1 Å, therefore it is assumed as one layer) and Li layer (with lateral distance between Ti-O and Li layer equal 1.04 Å), the next lateral Ti-O layer (with distance 2.08 Å from previous Ti-O layer). The LFPO (100) surface is constructed by lateral Fe-O layer (lateral distance between O and Ti is equal 0.58 Å), P-O layer and Li layer (with lateral distance between P and Li layer equal 1.0 Å and Fe and Li layer equal 2.25 Å). The adsorption of both adsorbates (DMC and EC) via carbonyl oxygen has been considered at all four clusters, L4TO, L7TO, FPO, and LFPO (see Figure S6 and S7c and S7f). The both adsorbates are adsorbed at angular positions at M centers (M = Ti or Fe): DMC as bidentate adsorbate at L4TO and L7TO (bind with 2 Ti centers) as well as monodentate adsorbate at FPO and LFPO and EC as monodentate adsorbate (bind with single Ti or Fe center).

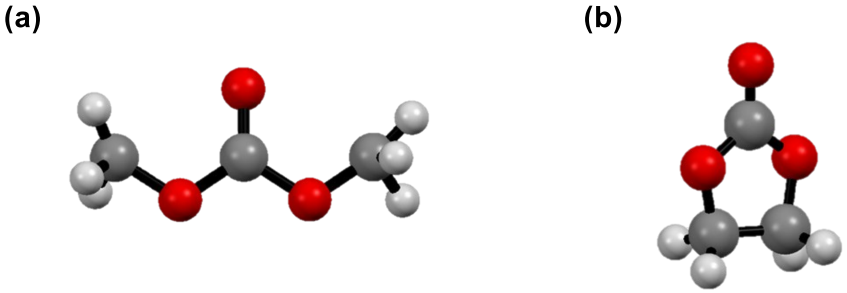

Fig. S5. Optimized structures of the organic solvents used in this DFT study, (a) Dimethyl Carbonate (DMC) [$C_3H_6O_3$], (B) Ethylene Carbonate (EC) [$(CH_2O)_2CO$].

(a) FPO

(b) LFPO

(c) DMC adsorbed on FPO

(d) DMC adsorbed on LFPO

(e) EC adsorbed on FPO

(f) EC adsorbed on LFPO

Fig. S6. Optimized structures of the clusters representing the structure of (a) non-lithiated $FePO_4$ (FPO), (b) lithiated $LiFePO_4$ (LFPO), and the structures of the adsorbed DMC on FPO (c) and LFPO (d) and the adsorbed EC on FPO (e) and LFPO (f) via carbonyl group.

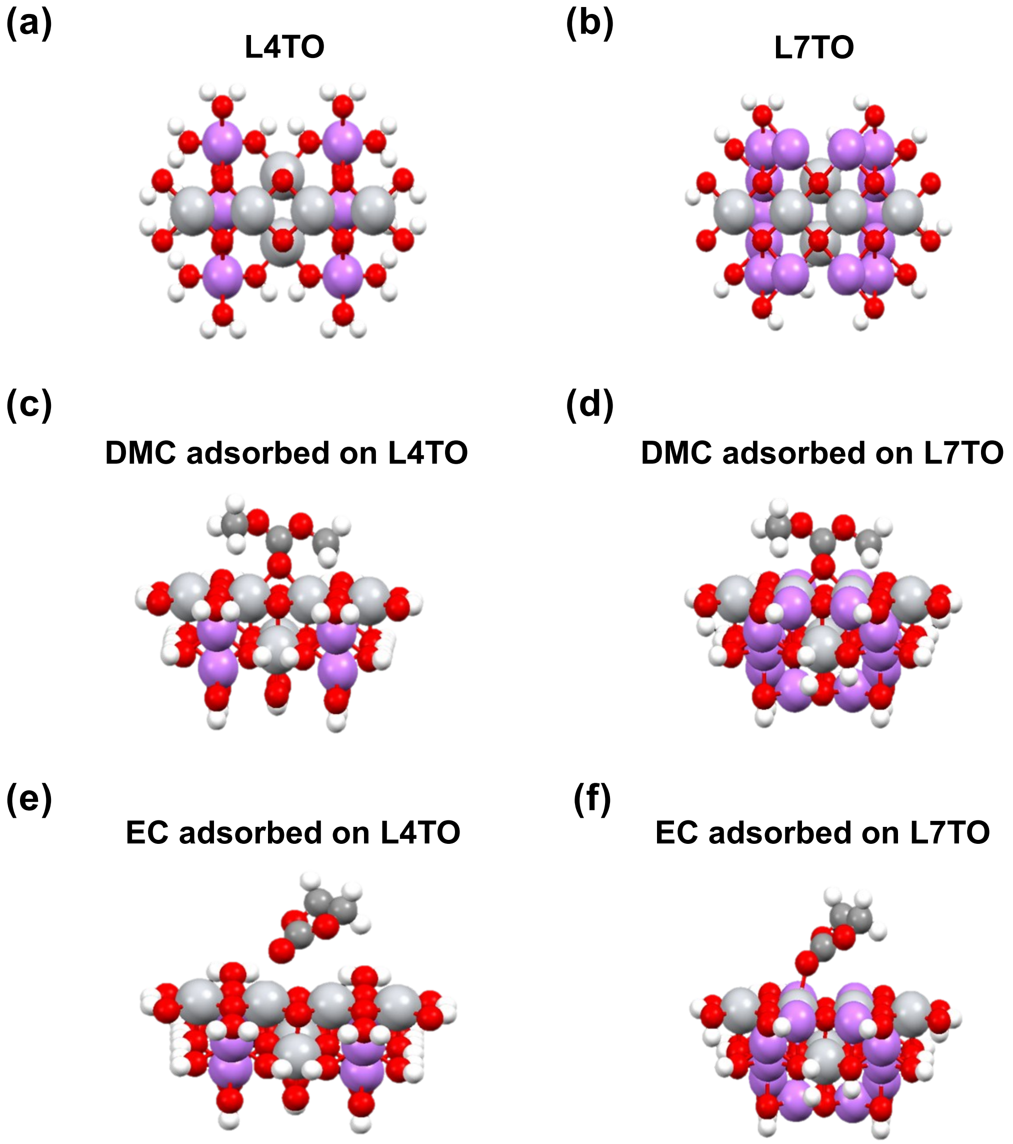

Fig. S7. Optimized structures of the clusters representing the structure of (a) non-lithiated $Li_4Ti_5O_{12}$ (L4TO), (b) lithiated $Li_7Ti_5O_{12}$ (L7TO), and the structures of the adsorbed DMC on L4TO (c) and L7TO (d) and the adsorbed EC on L4TO (e) and L7TO (f) via carbonyl group.

Detailed analysis of the total density of states (tDOS) as well as the partial, atom projected, density of states (pDOS) of isolated systems and the adsorbed solvents on cathode and anode surfaces are performed (Figure S8 and S9), with a FWHM equal 0.2 eV. The virtual orbitals are included above the Fermi level to visualize the LUMO orbitals. Only central atoms have been included to the DOS to avoid the effect of peripheral atoms (e.g. artificial hydroxyl bonds effect).

In the main manuscript and in the supporting information document, the nomenclature HOMO and LUMO referred to the highest occupied molecular orbital and lowest unoccupied molecular orbital respectively, were used for organic molecular structures e.g. DMC and EC. However, the nomenclature valence band (VB) and conductive band (CB) were used for inorganic structures e.g. L4TO/L7TO and LFPO/FPO. It is worth to notice that, the position of the VB extracted from the DOS is estimated based on electrodes at open circuit potential (OCP) state. To simplify our model and the comparison between the different lithiation and delithiation states of the electrodes, we estimated the Fermi level (FL) at the same position of the VB. The alignment of the different DOS were conducted by setting the FL of FPO and L4TO to 0 eV, for that we shifted all DOS by 4.45 eV and 5.41 eV based on FPO and L4TO's valence band levels, respectively (Table S1 and S2). However, during lithiation and delithiation of the electrodes (the so called operating potential in the manuscript) the FL is expected to shift until the electrodes reach the plateaus potentials of 1.55 V vs. Li^+/Li for L4TO and 3.45 V vs. Li^+/Li for LFPO. The FL shifts applied in Figure 4 (in the manuscript) at operating potential is 1.45 V to higher energy and 0.5 V to lower energy for L4TO and LFPO respectively. Those shifts are estimated by considering the OCP potentials of both L4TO and LFP equal to ~3 V vs. Li^+/Li. The difference between the OCP potentials and the operating potentials of both plateaus gives (3 V – 1.55 V = 1.45 V) for L4TO and (3V – 3.45 V = 0.45 V) for LFPO.

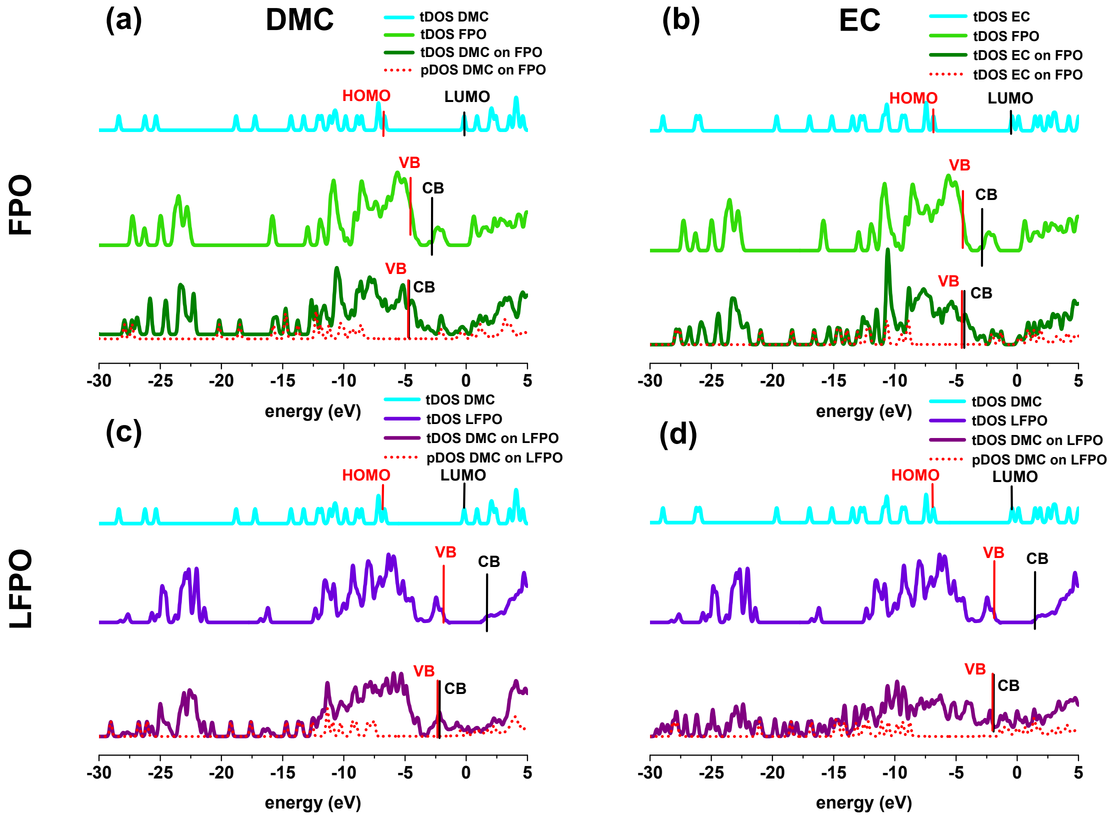

Fig. S8. Density of State (DOS) calculated for DMC and EC (cyan curves), non-lithiated $FePO_4$ (FPO - light green curves) and lithiated $LiFePO_4$ (LFPO - violet curves) as isolated systems. Total DOS (tDOS) of the adsorbed DMC and EC on FPO (dark-green curves in (a) and (b), respectively) and tDOS of adsorbed DMC and EC on LFPO (purple curves in (c) and (d), respectively). The partial DOS (pDOS) are reported for all the combined systems as dotted-red lines. HOMO and VB are evidenced with red lines for the solvent molecules and LFPO/FPO structures; LUMO and CB are delineated with black lines for solvent molecules and LFPO/FPO structures.

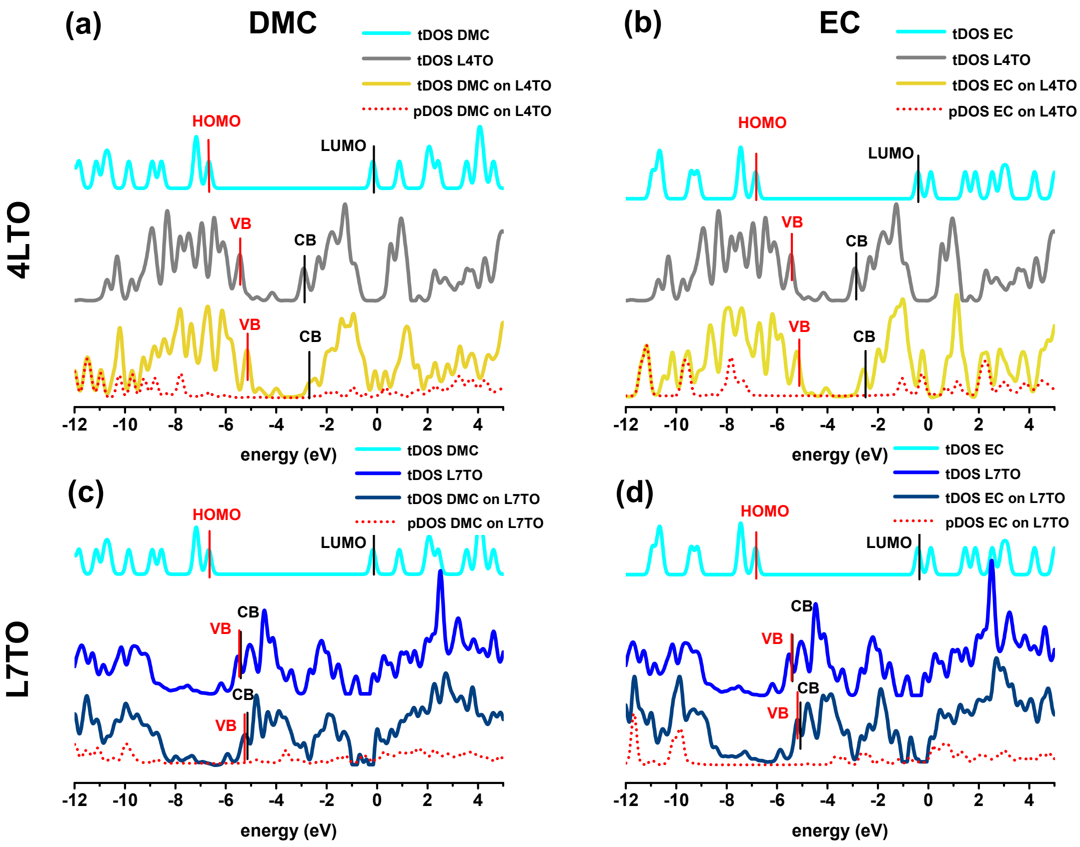

Fig. S9. Density of States (DOS) calculated for DMC and EC (cyan curves), non-lithiated $Li_4Ti_5O_{12}$ (L4TO - grey curves) and lithiated $Li_7Ti_5O_{12}$ (L7TO - blue curves) as isolated systems. Total DOS (tDOS) of the adsorbed DMC and EC on L4TO (yellow curves in (a) and (b), respectively) and tDOS of adsorbed DMC and EC on L7TO (dark-blue curves in (c) and (d), respectively). The partial DOS (pDOS) are reported for all the combined systems as dotted-red lines. HOMO and VB are evidenced with red lines for the solvent molecules and L4TO/L7TO; LUMO and CB are delineated with black lines for solvent molecules and L4TO/L7TO structures.

Table S1. (a) HOMO/LUMO and valence band (VB)/conductive band (CB) energies for the investigated structures before applying energies correction by shifting the FPO VB (-4.45 eV) to EF=0. (b) Offset energy ΔE between the HOMO of the DMC and EC solvents and the VB of the FPO and LFPO electrodes.

(a)

Structures	HOMO/VB [eV]	LUMO/CB [eV]	Diff. |HOMO-LUMO| [eV]
DMC	-6.68	-0.17	6.51
EC	-6.85	-0.41	6.44
FPO	-4.45	-2.7	1.75
LFPO	-1.9	1.48	3.38
DMC + FPO	-4.76	-4.7	0.06
DMC + LFPO	-2.22	-2.19	0.03
pDOS DMC on FPO	-8.55	-2.02	6.53
pDOS DMC on LFPO	-7.57	-0.46	7.11
EC on FPO	-4.53	-4.45	0.08
EC on LFPO	-1.95	-1.92	0.03
pDOS EC on FPO	-8.94	-2.12	6.82
pDOS EC on LFPO	-8.79	-1.39	7.40

(b)

ΔE	Offset |HOMOsolvents – VB cathode|	
	FPO	LFPO
DMC	2.23 eV	4.78 eV
EC	2.4 eV	4.95 eV
Adsorbed DMC	3.79 eV	5.35 eV
Adsorbed EC	4.41 eV	6.84 eV

Table S2. (a) HOMO and LUMO energies for the investigated structures before applying energies correction by shifting the L4TO VB (-5.41 eV) to EF=0. (b) Offset energy ΔE between the LUMO of the DMC and EC solvents and the VB of the L4TO and L7TO electrodes.

(a)

Structures	HOMO/VB [eV]	LUMO/CB [eV]	Diff. │HOMO-LUMO│ [eV]
DMC	-6.68	-0.17	6.51
EC	-6.85	-0.41	6.44
L4TO	-5.41	-2.88	2.53
L7TO	-5.44	-5.42	0.02
DMC + L4TO	-5.12	-2.58	2.54
DMC + L7TO	-5.21	-5.13	0.08
pDOS DMC on L4TO	-6.08	-2.07	4.01
pDOS DMC on L7TO	-8.65	-4.87	3.78
EC on L4TO	-5.15	-2.48	2.67
EC on L7TO	-5.17	-5.12	0.05
pDOS EC on L4TO	-7.43	-1.07	6.36
pDOS EC on L7TO	-9.86	-4.82	5.04

(b)

ΔE	Offset │LUMO solvents – VB anode│	
	L4TO	L7TO
DMC	5.24 eV	5.27 eV
EC	5 eV	5.03 eV
Adsorbed DMC	3.05 eV	0.34 eV
Adsorbed EC	4.08 eV	0.35 eV

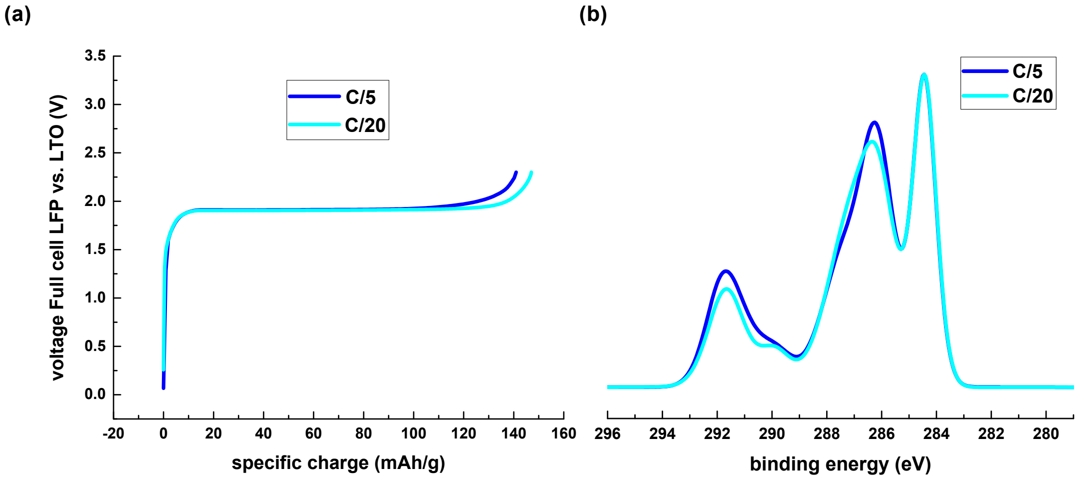

Fig. S10. (a) Galvanostatic curves of the 1st lithiation (charge) of L4TO (vs. LFPO) at two different cycling rates C/5 (dark blue) and C/20 (light blue). (b) XPS C1s core level acquired on two L4TO electrodes after the 1st lithiation at C/5 (dark blue) and C/20 (light blue).

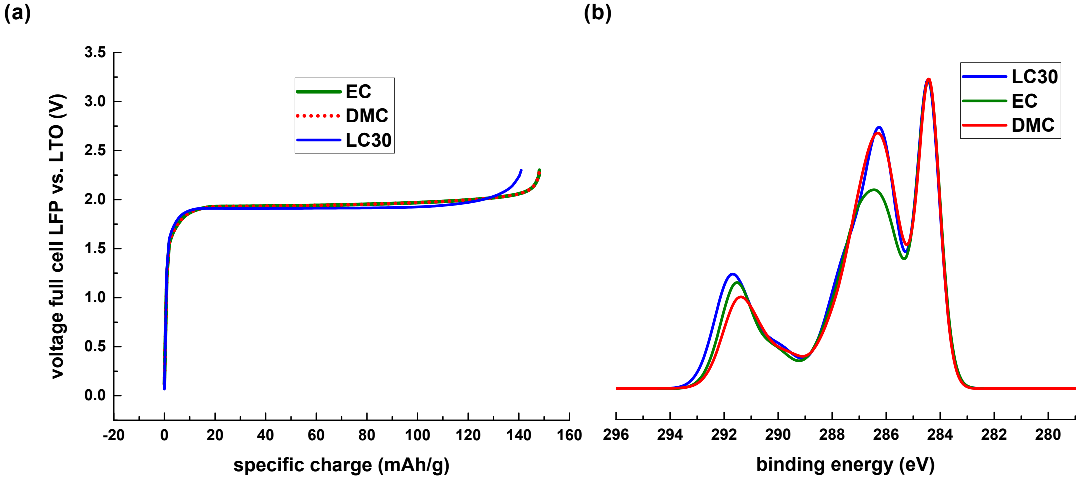

Fig. S11. (a) Galvanostatic curves at C/5 of the 1st lithiation **(**charge**)** of L4TO (vs. LFPO) using three different electrolytes of 1M LiClO$_4$ dissolved in pure EC (dark green), pure DMC (red dashed line) and EC:DMC, 1:1 (dark blue). (b) XPS C1s core level acquired on three L4TO electrodes after the 1st lithiation at C/5 in three different electrolytes. The electrodes formulation is 80% active materials, 10% conductive carbon and 10% PVdF binder.

Table S3. Adsorption energies [eV] for adsorbates on the investigated structures.

Adsorbate	**FPO**	**LFPO**	**L4TO**	**L7TO**
DMC	-1.71	-0.49	-2.64	-2.11
EC	-1.94	-0.45	-0.48	-0.98